



OPEN

SUBJECT AREAS:

MECHANISMS OF
DISEASE

ANIMAL DISEASE MODELS

OPTICAL IMAGING

GLOMERULUS

Received
22 May 2013Accepted
9 December 2013Published
27 January 2014

Correspondence and requests for materials should be addressed to A.D.K. (andreas.kistler@usz.ch) or A.F. (afornoni@med.miami.edu)

In vivo imaging of kidney glomeruli transplanted into the anterior chamber of the mouse eye

Andreas D. Kistler^{1,2}, Alejandro Caicedo³, Midhat H. Abdulreda⁴, Christian Faul¹, Dentscho Kerjaschki⁵, Per-Olof Berggren^{4,6}, Jochen Reiser^{1,7} & Alessia Fornoni^{1,4}

¹Department of Medicine, Division of Nephrology and Hypertension, University of Miami Miller School of Medicine, Miami, Florida, USA, ²Division of Nephrology, University Hospital Zürich, Zürich, Switzerland, ³Department of Medicine, Division of Endocrinology, Diabetes and Metabolism, University of Miami Miller School of Medicine, Florida, USA, ⁴Diabetes Research Institute, Miller School of Medicine, University of Miami, Miami, Florida, ⁵Clinical Institute of Pathology, Medical University of Vienna, Vienna, Austria, ⁶The Rolf Luft Research Center for Diabetes and Endocrinology, Karolinska Institutet, Stockholm, Sweden, ⁷Department of Medicine, Rush University Medical Center, Chicago, IL, USA.

Multiphoton microscopy enables live imaging of the renal glomerulus. However, repeated *in vivo* imaging of the same glomerulus over extended periods of time and the study of glomerular function independent of parietal epithelial and proximal tubular cell effects has not been possible so far. Here, we report a novel approach for non-invasive imaging of acapsular glomeruli transplanted into the anterior chamber of the mouse eye. After microinjection, glomeruli were capable of engrafting on the highly vascularized iris. Glomerular structure was preserved, as demonstrated by podocyte specific expression of cyan fluorescent protein and by electron microscopy. Injection of fluorescence-labeled dextrans of various molecular weights allowed visualization of glomerular filtration and revealed leakage of 70 kDa dextran in an inducible model of proteinuria. Our findings demonstrate functionality and long-term survival of glomeruli devoid of Bowman's capsule and provide a novel approach for non-invasive longitudinal *in vivo* study of glomerular physiology and pathophysiology.

The kidney's basic filtration unit, the glomerulus, ensures highly size-selective ultrafiltration of blood. In an average adult human, the kidneys produce 180 liters of primary urine every day, yet loss of proteins into the urine is negligible, primarily due to size selectivity of the glomerular filter. This remarkable task is accomplished by an elaborate structure of the three-layered glomerular filtration barrier consisting of a glomerular endothelium on the inside of the glomerular capillaries, a specialized glomerular basement membrane and interdigitating podocyte foot processes on the outside¹. Our knowledge of glomerular structure and function has grown tremendously in the past few decades, yet several critical questions remain unresolved and cause ongoing debate, such as the exact glomerular permeability for albumin^{2–4}. Recent advances in imaging technologies have allowed the visualization of dynamic processes *in vivo*⁵, thus complementing previous morphologic studies largely based on fixed tissue, as well as mechanistic studies that were mostly based on *ex vivo* micro-manipulation techniques, such as micropuncture and microperfusion. However, due to the intricate functional interplay of the glomerular tuft with Bowman's capsule (a sac-like structure consisting of a single layer of parietal epithelial cells that comprise the glomerular tuft) and the proximal tubular epithelium, even advanced *in vivo* imaging modalities of the intact kidney do not always allow functional studies of the glomerular filter independent of surrounding structures. In particular, it has not been possible to study glomerular function in the absence of parietal epithelial cells and proximal tubular function to thus specifically address the contribution of these structures to glomerular function. Furthermore, existing imaging techniques do not allow for long-term repetitive studies in the same living animal, even less so of the same glomerulus. Therefore, additional complementary approaches to study glomerular function are needed. Here, we describe a novel approach to study glomerular function by repetitive non-invasive *in vivo* imaging of isolated glomeruli transplanted into the anterior chamber of the mouse eye.

The anterior chamber of the mouse eye has been previously used as a site to transplant tissue⁶, including pancreatic islets⁷, as well as whole embryonic kidneys⁸. The iris provides a favorable environment for engraftment due to its high vascularization, and the cornea functions as a natural body window for *in vivo* imaging of



transplanted tissue non-invasively and longitudinally. We, therefore, wondered whether glomeruli injected into the anterior chamber of the mouse eye would be capable to engraft on the iris and gain access to the iris vasculature. Here, we demonstrate that a fraction of injected glomeruli engraft on the iris, can be repeatedly imaged over time and maintain filtration capability and preserved podocyte structure even in the absence of parietal epithelial cells. We suggest that this simple transplantation model may be useful to study certain aspects of glomerular function and we present preliminary data on potential applications.

Results

Engraftment and perfusion of transplanted glomeruli. Donor mice were perfused with isotonic crystalloid solution via the left ventricle. Immediately thereafter, kidneys were harvested and glomeruli were isolated by sequential sieving followed by manual microdissection to obtain pure glomeruli devoid of contaminations by renal tubuli. A capsular glomeruli were then injected via a blunt eye-cannula through a small incision in the corneal limbus into the anterior chamber of anesthetized recipient mice, where they settled and attached to the iris (Fig. 1a). We used Rag-2 deficient mice lacking mature T- and B-lymphocytes⁹ as recipients to prevent rejection of transplanted glomeruli derived from allogeneic donors. Transplanted glomeruli were imaged in anesthetized recipient mice using a head constraint (Fig. 1b), and were easily visible at 5× magnification (Fig. 1c). The majority of transplanted glomeruli appeared to collapse and slowly decomposed on top of the iris over the course of several weeks. However, some gained access to the iris vasculature and became reperfused within two weeks after transplantation. Perfusion of engrafted glomeruli was demonstrated by tail vein injection

of high molecular weight (2,000 kDa) fluorescently labeled dextran, which remains strictly intravascular, and imaging using a water-immersion 20× magnification lens for confocal laser-scanning microscopy (Fig. 1d and three dimensional reconstruction in Supplementary movie 1). Note the green fluorescence of recipient endothelial cells contributing to the revascularization of the transplanted glomeruli (see below). Supplementary movie 2 shows real-time imaging of a transplanted glomerulus after injection of 70 kDa dextran, which also remained intravascular.

Survival of differentiated podocytes in transplanted glomeruli. To visualize podocytes and determine their viability after transplantation, we used donor mice expressing cyan fluorescent protein (CFP) under the control of the podocyte-specific NPHS1 promoter¹⁰. The NPHS1 (nephrin) promoter is specifically expressed in differentiated glomerular podocytes and its expression is lost in several pathological situations as well as during dedifferentiation of podocytes in primary cell culture. Transplanted glomeruli retained their differentiated podocytes as indicated by continued CFP expression, which could be easily visualized by blue fluorescence of glomeruli from NPHS1-CFP mice that was completely absent in glomeruli from mice not transgenic for NPHS1-CFP (Fig. 2). A three dimensional reconstruction of an engrafted glomerulus with podocytes visualized by blue fluorescence is shown in Supplementary movie 3. We next verified preservation of the interdigitating podocyte foot processes by electron microscopy (Fig. 3a and b) and confirmed expression of the podocyte marker podocalyxin by immunogold electron microscopy (Fig. 3c). Individual transplanted glomeruli were repeatedly imaged over time up to six months after transplantation and retained their structure, including differentiated (i.e. CFP expressing) podocytes throughout this time. Once engrafted and reperfused, glomeruli

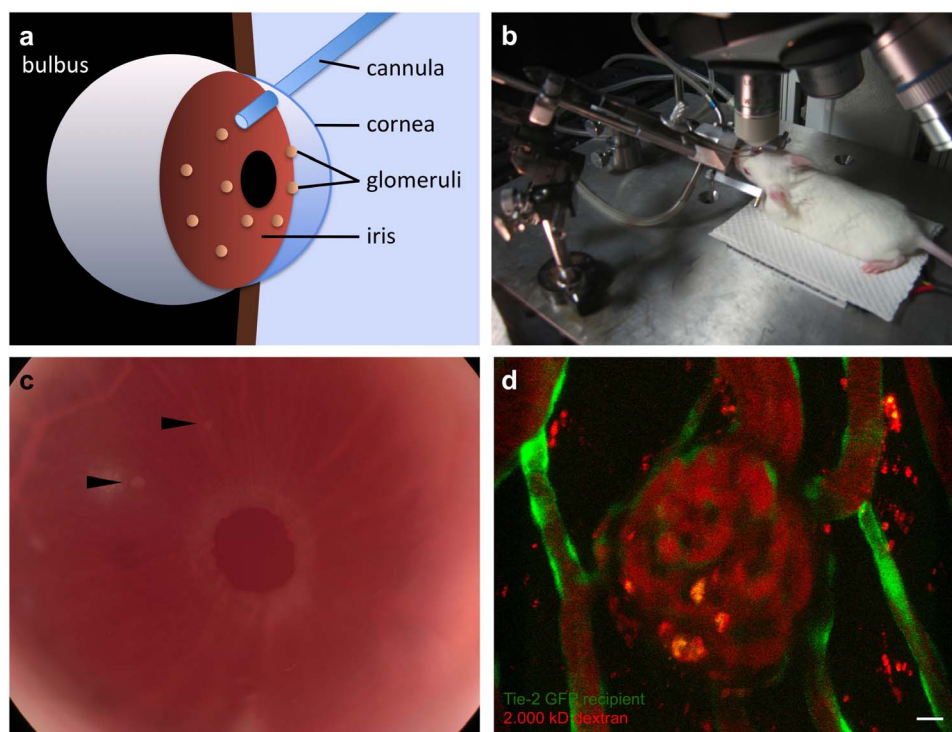


Figure 1 | Imaging of isolated mouse glomeruli transplanted into the anterior chamber of the mouse eye. (a) Schematic drawing of the transplantation procedure of isolated glomeruli into the anterior chamber. (b) For microscopic imaging, recipient mice were anesthetized and restrained with a stereotactic head holder with the transplanted eye facing the objective. (c) Transplanted glomeruli attached to the iris are detectable by low magnification microscopy. (d) Imaging of an engrafted glomerulus after tail vein injection of tetramethylrhodamine-labeled 2,000 kDa dextran (red) into the recipient mouse revealing perfusion of the transplanted glomerulus. Endothelial cell-specific expression of GFP (green) in the recipient (but not the donor) mouse reveals contribution of recipient endothelial cells to the capillary walls of the transplanted glomerulus. Shown is a maximum projection of a Z-stack of confocal images. Scale bar, 10 μ m.

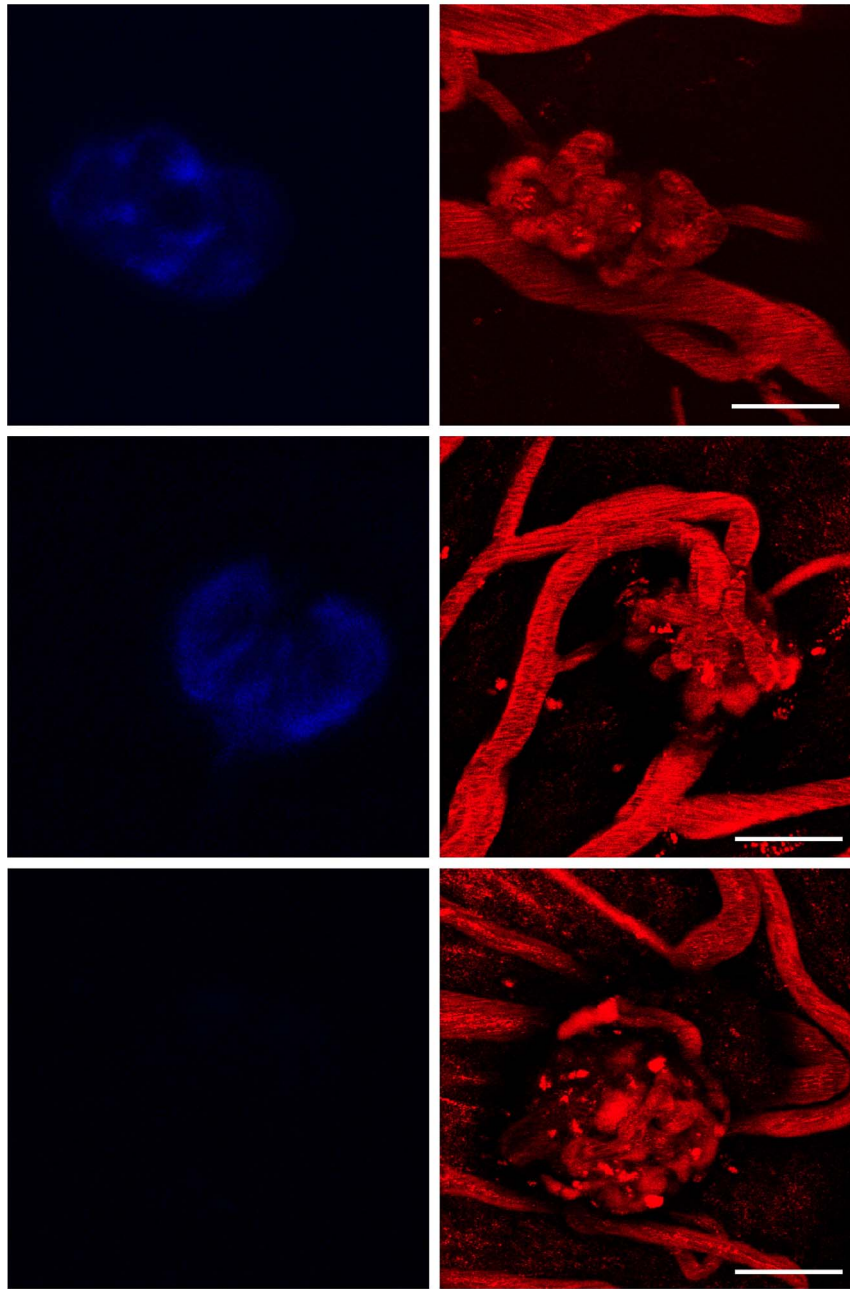


Figure 2 | Podocyte-specific expression of cyan fluorescent protein helps visualizing transplanted podocytes and reveals continued nephtrin expression. Transplanted glomeruli from donor mice that express cyan fluorescent protein under the NPHS1 (nephtrin)-promoter exhibit blue fluorescence (upper two rows), which was completely absent in negative control glomeruli from wild type mice (lower row). NPHS1-CFP expression helps visualize transplanted podocytes and demonstrates continued nephtrin expression by podocytes of transplanted glomeruli. Scale bar, 50 μ m.

did not show signs of degeneration and their size remained stable over time (Fig. 4).

Recipient endothelial cells contribute to the filtration barrier of transplanted glomeruli. It has been shown in transplanted pancreatic islets that the vascular endothelium of engrafted islets is derived from both, the donor and recipient animal¹¹. We therefore examined the contribution of recipient endothelial cells to the structure of the glomerular graft. Use of recipient mice expressing green fluorescent protein (GFP) under the endothelial Tie-2 promoter¹² demonstrated contribution of recipient endothelial cells to the filtration barrier of engrafted glomeruli (Fig. 1d, Supplementary movie 1 and Fig. 7).

Efficiency of the transplantation procedure. As noted above, only a fraction of transplanted glomeruli engrafted and became reperfused. In addition, some glomeruli showed only partial perfusion, i.e., of only one or few capillary loops (Fig. 5). In total, we have injected 36 eyes from 21 different mice with isolated glomeruli, and 5–20 glomeruli were injected per eye. Overall, 53 glomeruli in 22 transplanted eyes became reperfused, roughly half of them only partially. Hence, overall about 10% of transplanted glomeruli became completely reperfused. Of interest, podocyte survival did not depend on perfusion of the glomerular capillaries since unperfused areas of glomeruli, and even some entirely unperfused glomeruli retained blue fluorescence for several weeks (Fig. 5c). On the other hand, revascularization of transplanted glomeruli seems to

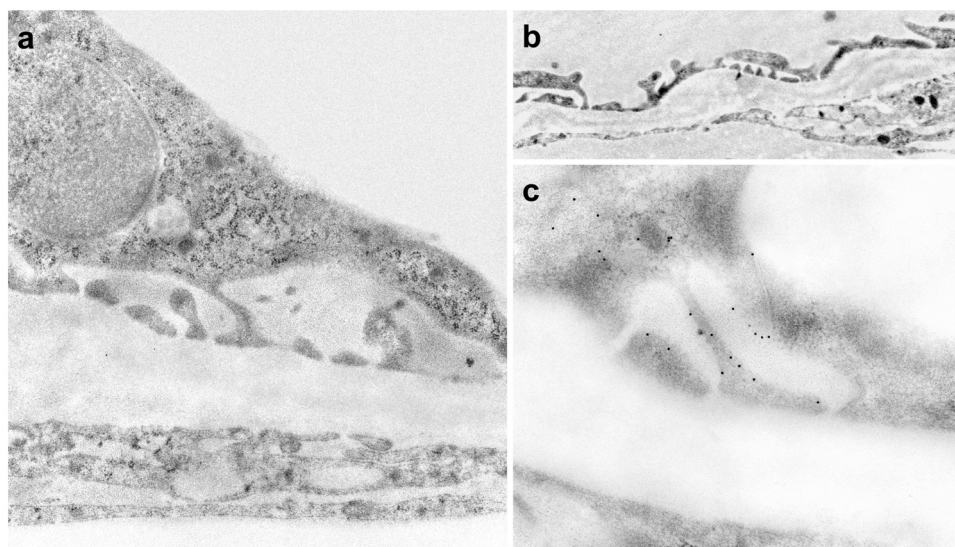


Figure 3 | Podocyte ultrastructure is preserved in glomeruli transplanted into the anterior chamber of the eye. (a) and (b) Transmission electron microscopy shows interdigitating podocyte foot processes. (c) Immunogold electron microscopy reveals conserved expression of podocalyxin in podocytes from transplanted glomeruli. Control sections stained with secondary antibody only were completely negative for gold particles.

depended on podocyte survival or differentiation since none of the glomeruli that had lost blue fluorescence (i.e., nephrin expression) within the first two weeks after transplantation became reperfused. This suggests that revascularization of transplanted glomeruli might depend on podocyte-secreted factors, such as vascular endothelial growth factor (VEGF)¹³.

Acapsular glomeruli show evidence of filtration. To study the functionality of transplanted glomeruli, we used fluorescence-labeled dextrans with various molecular weights. Injection of 2.000 kDa dextran, which strictly remains intravascular due to its large size, clearly delineates the intravascular space (Fig. 6a). Upon subsequent injection of low molecular weight (LMW) dextran (10 kDa) into the same mouse followed by imaging of the same glomerulus, a double-contour appeared, which indicated a larger volume of distribution for the LMW compared to the high molecular weight dextran (Fig. 6d). Simultaneous visualization of podocytes by blue fluorescence revealed a small gap between the intravascular space and the podocytes, which was inaccessible to the high molecular

weight dextran but subsequently filled by the LMW dextran (Fig. 6b, c, e and f). This space, situated between the capillary lumen and podocyte cell bodies, most likely represents the subpodocyte space¹⁴. Simultaneous visualization of CFP-expressing podocytes (blue) and GFP-expressing endothelium (green) confirmed localization of the subpodocyte space between the filtration barrier and podocyte cell bodies (Fig. 7). Quantification of fluorescence across the glomerular capillary wall further revealed slightly increased fluorescence outside the capillary wall (Fig. 6g), indicating filtration of the dye, which is most likely rapidly diluted in the aqueous humor. As shown in Supplementary movie 4, 10 kDa dextran appears in the subpodocyte space immediately after dye injection, thus demonstrating filtration rather than diffusion of the dextran.

Detection of increased glomerular permeability in an inducible genetic model of podocyte injury. Because we were able to image glomerular filtration, we hypothesized that glomerular proteinuria might be visualized by detecting leakage of labeled 70 kDa dextran.

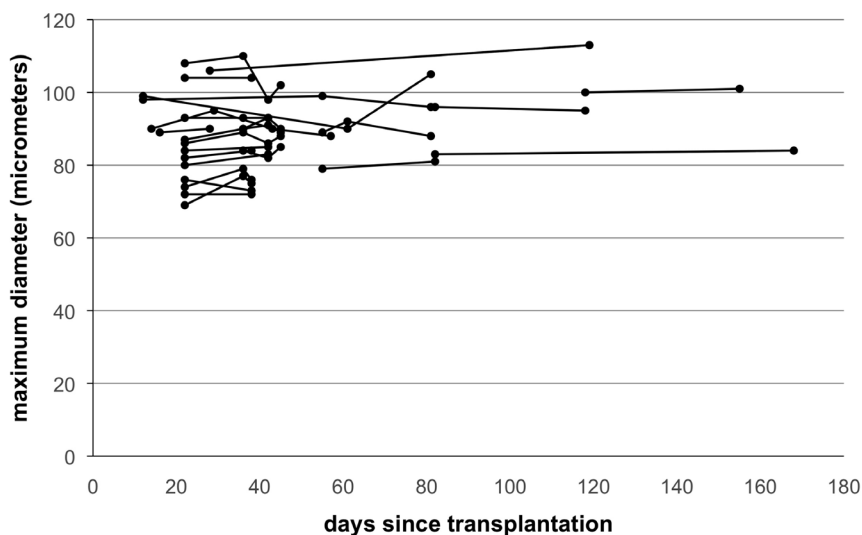


Figure 4 | Diameter of glomeruli imaged repeatedly over time. The maximum diameter of individual glomeruli that have been repeatedly imaged over time is shown. Note the stable size of glomeruli over time.

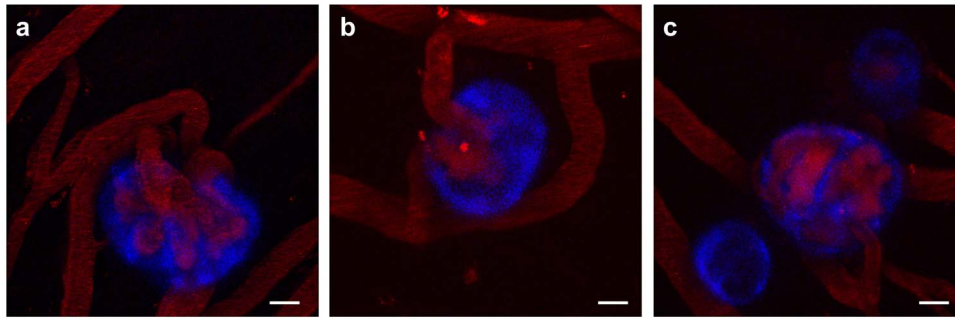


Figure 5 | Examples of transplanted glomeruli with complete or partial reperfusion. Shown are maximum projections of z-stacks acquired by confocal laser scanning microscopy. (a) Example of an engrafted glomerulus that became entirely reperfused. (b) Example of a glomerulus where only one capillary loop became reperfused. (c) Group of three transplanted glomeruli of which only one became perfused. Note that podocytes survived (as demonstrated by continuous expression of CFP under the control of the NPHS1 promoter) in two glomeruli despite the lack of revascularization (lower left and upper right glomerulus). Scale bars, 10 μm .

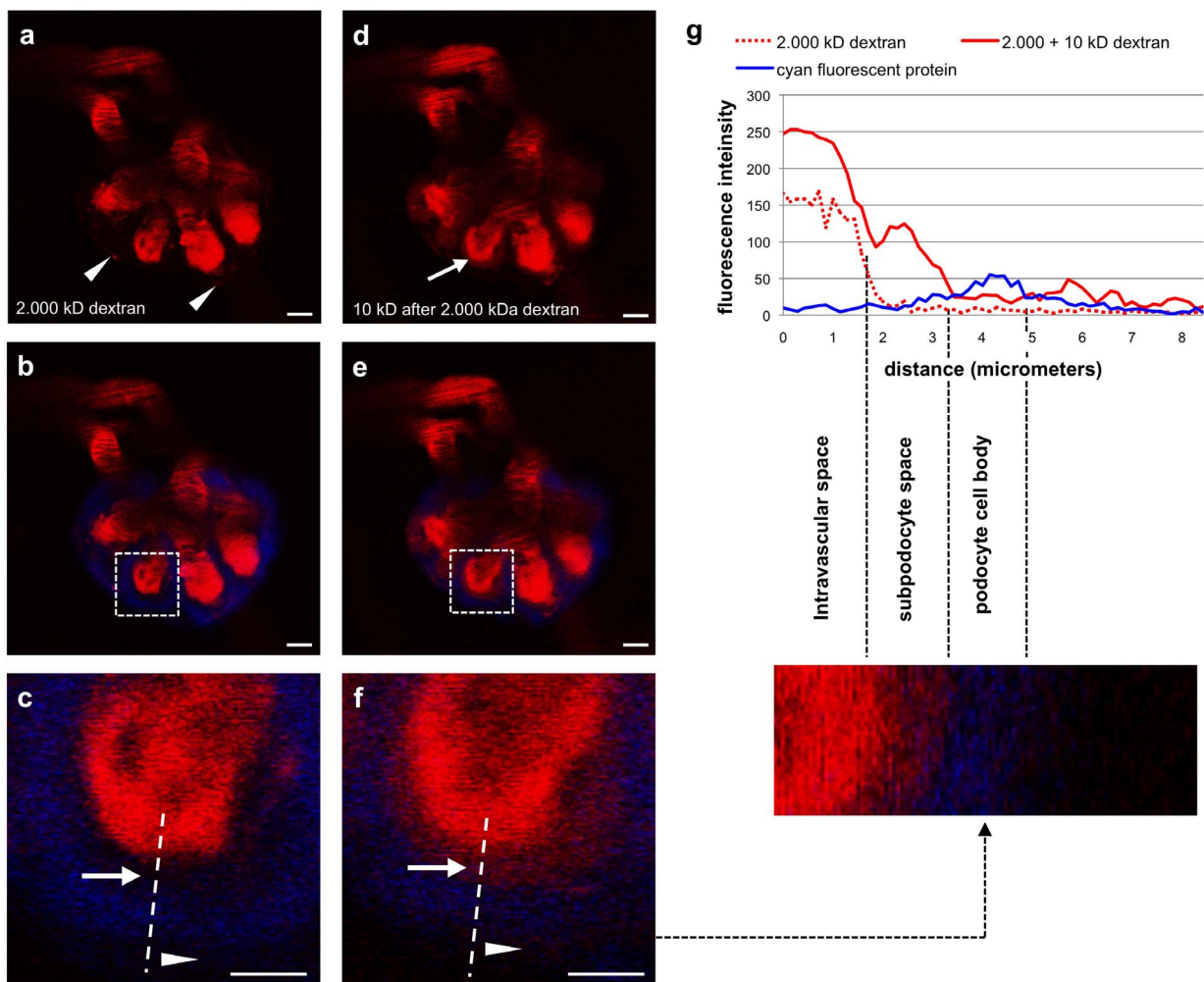


Figure 6 | 10 kDa dextran is filtered by transplanted glomeruli and suggests the presence of a subpodocyte space. (a–c) Injection of 2000 kDa dextran served to delineate the intravascular space. Simultaneous visualization of podocytes expressing CFP (blue fluorescence in b and c) reveals a small gap between the intravascular space and podocyte cell bodies (arrow in c). The faint red fluorescence within the outer aspect of podocytes (arrowheads in a) was present before injection of the 2000 kDa dextran and most likely results from endocytosis of labeled dextran from previous injections in the same mouse. (d–f) Injection of 10 kDa dextran in the same mouse ~10 minutes after injection of the 2000 kDa dextran reveals filtration of 10 kDa dextran into the subpodocyte space resulting in a double contour of glomerular capillaries (d; note that intravascular fluorescence in (d–f) represents the sum of the previously injected 2000 kDa dextran and the 10 kDa dextran). Filtered 10 kDa dextran fills the gap between the intravascular space and podocyte cell bodies (arrow in f). Only minimal fluorescence is visible outside the subpodocyte space directly after injection of the 10 kDa dextran (arrowhead in f vs. arrowhead in c) suggesting rapid dilution of the dextran once it leaves the subpodocyte space. (g) Quantification of the red (dextran) and blue (podocyte CFP) fluorescence intensities along a cross section of the capillary (dashed lines in panels c and f). Scale bars = 10 μm (a), (b), (d) and (e) or 5 μm (c) and (f).

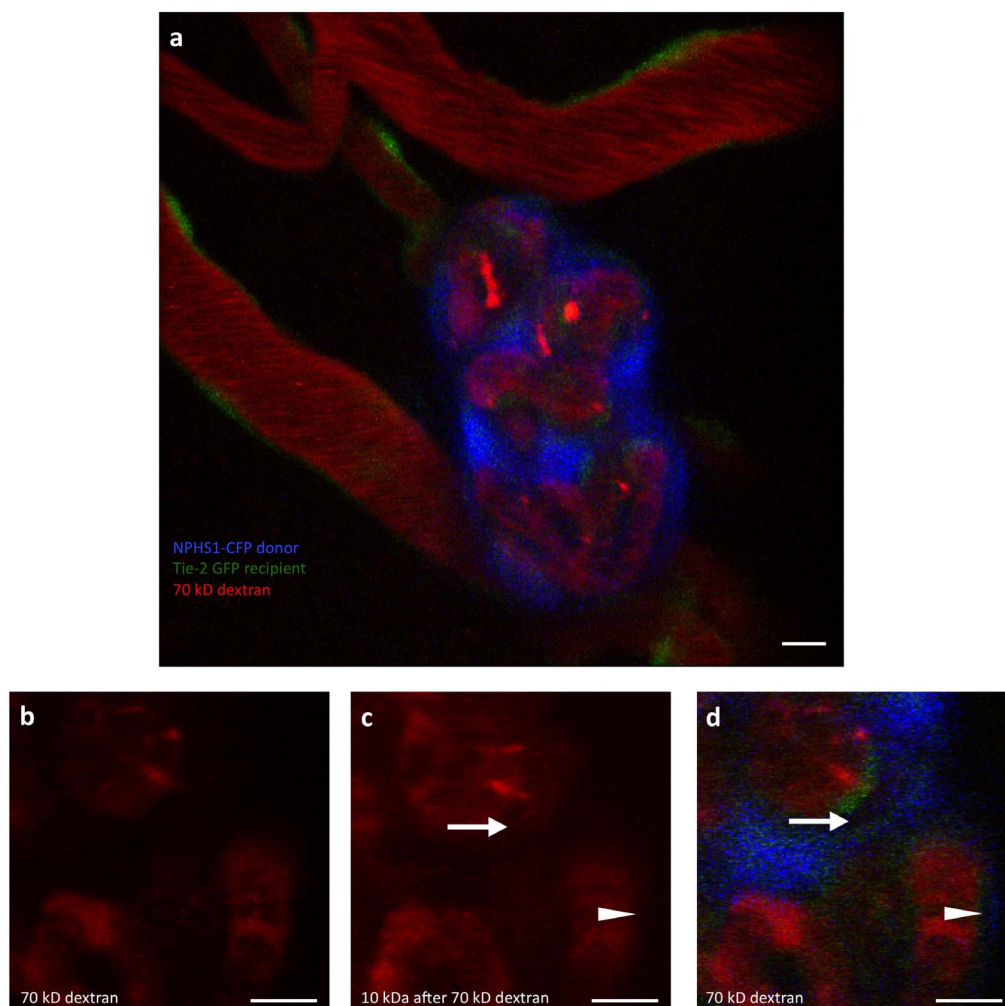


Figure 7 | Simultaneous visualization of donor-derived podocytes and recipient-derived endothelial cells. (a) Maximum projection of a z-stack acquired by confocal laser scanning microscopy of a glomerulus from a donor mouse with podocyte-specific expression of cyan fluorescent protein into a recipient mouse with endothelial cell specific expression of green fluorescent protein. The image was acquired at day 186 after transplantation. Fluorescently labeled 70 kDa dextran remains confined to the intravascular space. (b) Detail from image (a) showing the red channel only. (c) Subsequent injection of 10 kDa dextran in the same mouse reveals filtration of the low molecular weight dextran with some accumulation next to the intravascular space. (d) Simultaneous visualization of podocytes (blue) and recipient-derived endothelial cells (green) confirms localization of the inter- (arrow in c and d) and subpodocyte space (arrowhead in c and d) between endothelial cells and podocytes. Note that separation of the CFP and the GFP signal is not perfect due to the overlapping emission spectra. Scale bars = 5 μ m.

We used double transgenic podocin-rtTA/TetO-HA-NFATc1^{fluc} donor mice which express constitutive active NFAT specifically in podocytes in an inducible manner and develop heavy proteinuria within seven days of oral doxycycline administration¹⁵. Glomeruli from doxycycline-naïve double transgenic mice were transplanted into wild type donors and three weeks after transplantation, transgene expression was induced specifically in transplanted podocytes by feeding recipient mice doxycycline-containing chow. Four transplanted glomeruli in two recipient mice were imaged longitudinally before and nine days after transgene induction (Fig. 8a). Fluorescence intensity plotted across the glomerular capillary wall five minutes after injection of 70 kDa dextran revealed its increased concentration in the subpodocyte space after doxycycline treatment (Fig. 8b, arrow), but not in doxycycline-insensitive recipient iris vessels (Fig. 8c, arrowhead). Quantification of fluorescence across eight capillary loops in four glomeruli of two mice demonstrated a significant increase of fluorescence intensity adjacent to the capillary wall (i.e. within the subpodocyte space) upon transgene induction. Fluorescence intensity was measured inside the glomerular capillary closely adjacent to the capillary wall excluding from the measure-

ments areas occupied by passing erythrocytes, as well as at a defined distance from the capillary wall (1.5 μ m from where the fluorescence intensity had decreased to 50% of the intracapillary intensity). After subtracting baseline fluorescence (from images acquired immediately before dextran injection), the fluorescence intensity outside the capillary wall was expressed as a percentage of the fluorescence intensity inside the capillaries, thus giving a measure of the percentage of 70 kDa dextran reaching the extracapillary space (i.e. the glomerular sieving coefficient, GSC). The GSC for 70 kDa dextran significantly increased from 0.035 to 0.095 upon induction of podocyte damage. This confirmed increased leakage of 70 kDa dextran through the glomerular capillaries in the disease model.

Discussion

Our data show that isolated acapsular glomeruli transplanted into the anterior chamber of the mouse eye are capable to spontaneously regain access to the recipient vasculature and retain their structure and function. We have thus developed a model to study with repetitive *in vivo* imaging the structure and function of acapsular glomeruli.

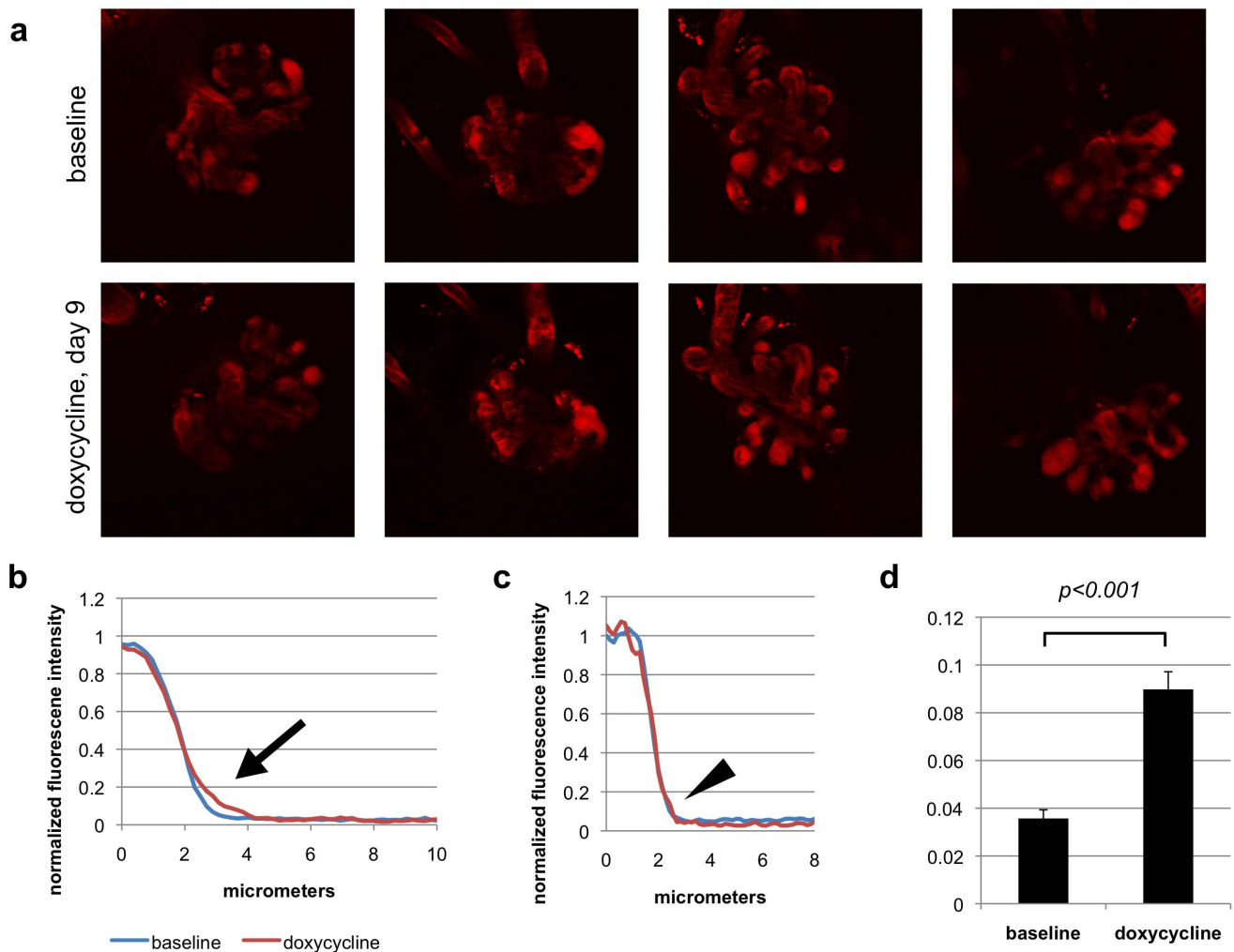


Figure 8 | Non-invasive *in vivo* visualization of glomerular proteinuria. The same glomeruli have been imaged upon tail vein injection of 70 kDa dextran before (panel (a), upper row) and nine days after (panel (a), lower row) doxycycline-induction of podocyte specific NFATc1^{trunc} transgene expression in transplanted glomeruli, which is known to cause podocyte foot process effacement and proteinuria. Fluorescence intensity was quantified along the capillary wall at several points and normalized to intracapillary fluorescence intensity. Plotting of fluorescence intensity against distance reveals increased intensity directly adjacent to the outside of the capillary when comparing baseline measurements (blue) to measurements after proteinuria induction (red) in glomerular capillaries (b); mean intensity of 8 capillary loops in 4 glomeruli of 2 mice plotted against the distance along the capillary cross section) but not in the doxycycline-resistant iris vasculature of the recipient ((c); intensity plot across an iris vessel). (d) The mean fluorescence intensity directly adjacent to the glomerular capillary wall of 8 capillary loops in 4 glomeruli of 2 mice significantly increased upon induction of podocyte damage with doxycycline-induced NFATc1^{trunc} transgene expression. Fluorescence intensity has been measured at a defined distance from the capillary wall (1.5 μm from where the fluorescence intensity had decreased to 50% maximum) and normalized to the maximum fluorescence intensity inside the glomerular capillary.

This model represents a novel approach to study several aspects of glomerular structure and function, which may complement established *in vivo* imaging methods, such as multiphoton microscopy in the exteriorized intact kidney¹⁶. Compared to the latter, despite being a more artificial system, our approach has some important strengths. It provides several technical advantages over imaging of the glomerulus in the intact kidney: it allows repetitive noninvasive imaging, whereas multiphoton microscopy in the intact kidney requires externalization of the kidney and cannot usually be performed repeatedly in the same animal over an extended period of time. Furthermore, due to the ideal optical properties of the cornea and the anterior chamber of the eye, imaging of transplanted glomeruli can be performed using conventional confocal laser scanning microscopy and does not necessarily require multiphoton microscopy equipment. Finally, the anterior chamber is easily accessible for manipulation, including the application of drugs and *in vivo* fluorescent dyes. Whereas small molecules may be applied as eye-drops and penetrate

the cornea, larger molecules, including fluorescence-labeled antibodies, can be microinjected into the anterior chamber to study and manipulate glomerular function, as described for transplanted pancreatic islets^{7,17}. In addition to these technical advantages, we have developed a simple transplantation model, which allows studying the roles and interplay of humoral factors and blood cells with resident glomerular cells of different genetic backgrounds. Since we demonstrated that recipient endothelial cells contribute to the glomerular filtration barrier of transplanted glomeruli, this model might also prove useful to study endothelial cell motility and turnover as well as podocyte-endothelial interactions during development and adulthood. Other future directions include the transplantation of glomeruli across species-barriers, including the transplantation of human glomeruli into mice. Using immune-deficient mice as recipients, human tissue has been previously successfully transplanted into the anterior chamber of the mouse eye⁶. Hence transplanting healthy or diseased human glomeruli into mouse eyes might in the future



represent the first possibility to image functioning human glomeruli *in vivo* and provide a means to study human glomerular diseases. This model may also allow to determine if some of the circulating biomarkers predictive of proteinuria have a causative role in disease pathogenesis.

Since we have transplanted glomeruli devoid of Bowman's capsule, our approach allows studying glomerular function in the absence of parietal epithelial cells. Parietal epithelial cells have been demonstrated to transmigrate from the parietal epithelium of Bowman's capsule along the glomerular vascular stalk and transdifferentiate into podocytes¹⁸. It is not known, however, whether continuous replacement of podocytes from parietal epithelial cells is necessary for the maintenance of glomerular function in ageing mice. Here, we demonstrate that acapsular glomeruli preserve their structure and function for at least six months after transplantation and that their size remains constant. Although the relatively low rate of glomeruli engraftment rendered a more detailed morphometric analysis of transplanted glomeruli not informative at this point, our data are sufficient to demonstrate that podocyte survival does not depend on the need for continuous replacement from parietal epithelial cells. In addition to their potential physiological roles, parietal epithelial cells participate in the formation of extracapillary proliferative lesions¹⁹ in crescentic glomerulonephritis as well as in sclerotic lesions in focal and segmental glomerulosclerosis (FSGS)²⁰, where adhesion of denuded glomerular basement membrane areas to the Bowman's capsule has been suggested to be a crucial initiating event²¹. Therefore, transplantation of acapsular glomeruli into the anterior chamber of the eye may provide a valuable model to determine if the presence of a Bowman's capsule is necessary for the development of histological lesions typical of FSGS and other glomerular diseases.

As mentioned above, our approach to study glomerular function certainly represents a highly artificial system. On one hand, the artificial nature of the system allows to study several particular aspects of glomerular physiology, as discussed above. On the other hand, however, transplanted glomeruli most likely do not behave in an entirely physiological way. It was therefore important to demonstrate the preservation of differentiated podocytes in transplanted glomeruli (as demonstrated by nephrin promoter activity driving CFP expression) and to confirm preserved podocyte foot process architecture (as demonstrated by electron microscopy). A limitation of our model is the fact that glomerular filtration pressure of transplanted glomeruli might be lower than that *in situ* in the kidney. Whereas intraglomerular pressure is assumed to approximate 40–50 mmHg, intracapillary pressure in most other capillaries is assumed to decrease from ca. 30 mmHg at the arterial to 20 mmHg at the venous side. The anterior chamber pressure is similar to the estimated pressure in Bowman's space (~15 mmHg), hence the pressure gradient for glomerular filtration might well be lower in transplanted glomeruli than *in situ*. Nevertheless the filtration pressure is positive and we were able to show evidence of glomerular filtration by injection of LMW dextran. The relatively low level of fluorescence detectable outside the glomerular capillaries upon injection of LMW dextran is probably due to the immediate dilution of filtered dye in the aqueous humor. The rapid appearance of the dextran in a space located between the podocytes and endothelial cells most likely represents retention of the filtered tracer in the subpodocyte space. This area, located between the outer aspect of the podocyte foot processes and podocyte cell bodies covering them¹⁴ has been previously suggested to restrict passage of the glomerular filtrate. Studies in freshly isolated, *ex vivo* perfused rat glomeruli have suggested restricted passage of 10 kD dextran through the sub-podocyte space²². Our data thus support a restrictive role of the subpodocyte space for glomerular filtration, which is not directly evident from *in vivo* studies in the intact kidney but can be visualized in our transplantation model through the immediate dilution in the aqueous

humor of dye leaving the subpodocyte space. Several questions regarding physiology of transplanted glomeruli remain to be answered, such as whether afferent and efferent arterioles can be transplanted with glomeruli, whether transplanted glomeruli retain autoregulation of perfusion and whether direction of blood flow in transplanted glomeruli is preserved or random. Future studies will address these open questions.

We provide preliminary evidence that our model system might be useful to study mechanisms of proteinuria *in vivo* by demonstrating increased glomerular leakage for 70 kD dextran in an inducible genetic model of podocyte damage. The GSC for 70 kDa dextran significantly increased upon the induction of podocyte damage, indicating damage to the glomerular filtration barrier. The baseline GSC for 70 kDa dextran in our studies was higher than in a different study in the intact kidney using two-photon microscopy²³ and clearly higher than the usually assumed GSC for the equally sized albumin^{24,25} but similar to a previously claimed value determined by two-photon microscopy² using labeled albumin. Since we used 70 kDa dextran as supplied by the manufacturer without prior size exclusion filtration, we cannot assume monodispersity of the dextran and our GSC values cannot be considered reliable estimates for the glomerular permeability to albumin or monodisperse 70 kDa dextran. Nevertheless, the significantly and clearly increased GSC for the dextran after disease induction demonstrates increased permeability of the glomerular filter and shows feasibility of this model to detect such an increase. Morphological analysis of glomeruli in the disease model is currently hampered by the low efficiency of transplantation (see below) and hence the difficulty to identify grafted and reperfused glomeruli (averaging one to three per eye) among other non-grafted glomeruli during histological preparation.

Entire fetal rat and mouse kidneys have previously been transplanted into the anterior chamber of rat⁸ and mouse²⁶ eyes and upon engraftment showed development of mature glomeruli. Our findings extend these interesting reports in several ways. First, in the cited reports, transplanted fetal kidneys contained only very early stages of developing nephrons that were avascular at the time of transplantation. Here, we show that mature glomeruli are capable of connecting to the recipient iris vasculature. Second, the transplantation of acapsular glomeruli allows the study of glomerular physiology in the absence of parietal epithelial cells and proximal tubuli, as discussed above. Finally, transplantation of isolated glomeruli allows easy visualization of glomerular physiology through *in vivo* fluorescence microscopy.

Engraftment occurred at a relatively low frequency, compared to the much higher efficiencies for the transplantation of other tissues, including pancreatic islets and fetal kidneys. This might be due to the fact that engraftment of pancreatic islets involves neovascularization and ingrowth of mostly recipient-derived capillaries⁷ into transplanted tissues, and developing glomeruli were still avascular in the case of fetal kidney transplantation⁸. This represents a fundamental difference to the transplantation of mature glomeruli, which are basically a tuft of capillaries and hence, their engraftment requires the formation of anastomoses between recipient iris vessels and pre-existing donor glomerular arterioles. It is thus noteworthy that isolated glomeruli have the capacity to attract recipient endothelial cells and to establish connections to the recipient vasculature. For a more widespread application, increasing the efficiency of engraftment would be desirable. Potential approaches include stimulation of endothelial growth by VEGF – either systemically injected or using transient inducible podocyte-specific overexpression²⁷ – as well as technical improvements of isolation and microinjection of glomeruli, including the injection of higher numbers of glomeruli per eye.

In summary, we have developed a novel approach to image and study the function of acapsular glomeruli *in vivo* over extended periods of time. Although this approach represents an artificial system, it may be particularly useful to investigate certain aspects of glomerular development, physiology and pathology *in vivo*.



Methods

Mouse models. We used as recipient mice Tie-2 GFP, Rag-2^{-/-}, NOD mice. These mice were generated by breeding the parental strains purchased from Jackson Laboratories. Tie-2 GFP mice express GFP under control of the endothelial-specific Tie-2 promoter, Rag-2^{-/-} mice are devoid of functioning B- and T-lymphocytes and thus do not reject allogeneic tissue grafts, and NOD mice were used due to their lack of pigmented iris epithelial cells, which might otherwise over time interfere with optical imaging. Because the development of diabetes mellitus in NOD mice depends on immunologic destruction of beta cells, Rag-2^{-/-} NOD mice are non-diabetic. Three donor mouse strains were used: 1) wild type C57BL/6 mice (purchased from Jackson Laboratories), 2) NPHS1-CFP mice¹⁰ kindly provided by Dr. Susan E. Quaggin (Samuel Lunenfeld Research Institute, Toronto, Canada) and 3) double transgenic doxycycline-inducible podocin-rtTA/TetO-HA-NFATc1^{nuc} mice¹⁵. Expression of constitutively active NFAT in transplanted glomeruli was induced by feeding recipient mice with chow containing doxycycline (2000 ppm; Research Diets) for nine days. All animal studies have been approved by the University of Miami Institutional Animal Care and Use Committee (IACUC).

Isolation and transplantation of glomeruli. Donor mice were perfused with Hank's buffered saline solution (HBSS) through the left ventricle to prevent thrombosis of glomerular capillaries after harvesting the kidneys. Kidneys were then harvested, cut into half, pressed through a sieve with 180 μm mesh size, sieved through a 100 μm sieve and collected in a 50 μm sieve. To achieve absolute purity from tubular contaminants, glomeruli were then manually collected with a micropipette tip coated with 1% bovine serum albumin (BSA). Isolated glomeruli were transferred to sterile PBS containing 1% BSA and aspirated into a blunt 27-gauge eye cannula connected to a 1-ml Hamilton syringe via polyethylene tubing. Under a stereomicroscope, we punctured the cornea of an isoflurane anesthetized recipient mouse close to the sclera with a 27-gauge needle, taking great care not to damage the iris. Next, we gently inserted the blunt cannula and slowly injected 5–20 glomeruli into the eye, where they slowly settled onto the iris. Transplanted mice recovered quickly and showed no signs of distress or irritation from the manipulated eye.

In vivo imaging of transplanted glomeruli. Mice were anesthetized using isoflurane and placed on a heating pad during imaging. The head was restrained with a stereotactic headholder and the eye containing the transplanted glomeruli was positioned upwards. The eyelid was carefully pulled back and the eye held gently with a pair of tweezers covered with polyethylene tubing. Imaging was performed using a Leica DMLFSA microscope with TCS-SP2-AOBS using a long-distance water-dipping objective (Leica HXC APO 20× 0.5 W) and PBS as immersion liquid. Fluorescently labeled dextrans (Invitrogen) were injected into the tail vein online while continuously imaging the mouse. Z-stacks of 512 × 512 pixels (0.1–0.75 μm per pixel) xy sections with 0.5- to 3-μm z-spacing were acquired using the resonant scanner, built into a Leica SP5 imaging system. Images were acquired in 8 bit mode for qualitative analysis (faster acquisition speed) and in 12 bit mode for quantitative analysis of 70 kDa dextran leakage in the inducible NFATc1^{nuc} model. For the quantification of glomerular permeability in the inducible NFATc1^{nuc} model, z-stack images were acquired immediately prior to the dextran injection to measure baseline background fluorescence and this value was subtracted from fluorescence values after dextran injection. Acquisition parameters were set such that intravascular fluorescence did not approach saturation. Three-dimensional (3D) renderings of z-stack images were done in Volocity software (Perkin Elmer, USA).

Quantification of glomerular permeability and statistical analysis. Fluorescence intensity was quantified using ImageJ software (NIH). Quantification was performed along six closely adjacent cross sections in the same glomerular capillary and mean values were calculated. For the quantification of 70 kDa dextran fluorescence across the capillary in the inducible NFATc1^{nuc} model, we analyzed a total of eight capillary loops of four glomeruli in two recipient mice, both before and after doxycycline treatment. To calculate the GSC, fluorescence levels at a defined distance from the glomerular capillary wall (1.5 μm from where the fluorescence intensity had decreased to 50% maximum) was divided by the intracapillary fluorescence, measured in areas not occupied by passing erythrocytes. Statistical comparisons were performed using two-sided student's T test.

Electron microscopy. Mouse eyes were perfusion-fixed with HBSS, followed by 4% PFA and 0.2% glutaraldehyde in ddH₂O via the left ventricle. The eyes were then enucleated, postfixed in 4% PFA and 0.2% glutaraldehyde in ddH₂O for 4 hours and subsequently kept in PBS 0.1% PFA at 4°C until further analysis. Fixed eyes were then dehydrated in 30%, 50%, 70%, 95% and 100% ethanol and embedded with lowicryl K4M (Polysciences, Inc, Gröpl), polymerized at minus 35°C and UV light. Ultrathin sections (about 80 nm) were collected on Formvar-carbon coated nickel grids and stained with 2% aqueous uranyl acetate and lead citrate. Immunoelectron microscopy was done essentially as described earlier²⁸. Briefly, Ultrathin sections were blocked with 1% ovalbumin in PBS for one hour, followed by incubation with affinity-purified goat antibody to podocalyxin (R&D, AF1556, 1:400) and an anti-goat 10 nm gold conjugate (1:50). Sections were counterstained with lead citrate. Sections stained with secondary antibody only served as negative controls and did not exhibit any staining.

- Haraldsson, B., Nystrom, J. & Deen, W. M. Properties of the glomerular barrier and mechanisms of proteinuria. *Physiol Rev* **88**, 451–487, doi:10.1152/physrev.00055.2006 (2008).
- Russo, L. M. *et al.* The normal kidney filters nephrotic levels of albumin retrieved by proximal tubule cells: retrieval is disrupted in nephrotic states. *Kidney Int* **71**, 504–513, doi:10.1038/sj.ki.5002041 (2007).
- Christensen, E. L., Birn, H., Rippe, B. & Maunsbach, A. B. Controversies in nephrology: renal albumin handling, facts, and artifacts! *Kidney Int* **72**, 1192–1194, doi:10.1038/sj.ki.5002526 (2007).
- Russo, L. M., Sandoval, R. M., Brown, D., Molitoris, B. A. & Comper, W. D. Controversies in nephrology: response to 'renal albumin handling, facts, and artifacts'. *Kidney Int* **72**, 1195–1197, doi:10.1038/sj.ki.5002528 (2007).
- Peti-Peterdi, J. & Sipos, A. A high-powered view of the filtration barrier. *J Am Soc Nephrol* **21**, 1835–1841, doi:10.1681/asn.2010040378 (2010).
- Speier, S. *et al.* Noninvasive high-resolution in vivo imaging of cell biology in the anterior chamber of the mouse eye. *Nat Protoc* **3**, 1278–1286, doi:10.1038/nprot.2008.118 (2008).
- Speier, S. *et al.* Noninvasive in vivo imaging of pancreatic islet cell biology. *Nat Med* **14**, 574–578, doi:10.1038/nm1701 (2008).
- Abrahamson, D. R., St John, P. L., Pillion, D. J. & Tucker, D. C. Glomerular development in intraocular and intrarenal grafts of fetal kidneys. *Lab Invest* **64**, 629–639 (1991).
- Shinkai, Y. *et al.* RAG-2-deficient mice lack mature lymphocytes owing to inability to initiate V(D)J rearrangement. *Cell* **68**, 855–867 (1992).
- Cui, S., Li, C., Ema, M., Weinstein, J. & Quaggin, S. E. Rapid isolation of glomeruli coupled with gene expression profiling identifies downstream targets in Pod1 knockout mice. *J Am Soc Nephrol* **16**, 3247–3255, doi:10.1681/asn.2005030278 (2005).
- Nyqvist, D. *et al.* Donor islet endothelial cells in pancreatic islet revascularization. *Diabetes* **60**, 2571–2577, doi:10.2337/db10-1711 (2011).
- Motoike, T. *et al.* Universal GFP reporter for the study of vascular development. *Genesis* **28**, 75–81 (2000).
- Eremina, V., Baelde, H. J. & Quaggin, S. E. Role of the VEGF--a signaling pathway in the glomerulus: evidence for crosstalk between components of the glomerular filtration barrier. *Nephron Physiol* **106**, p32–37, doi:10.1159/000101798 (2007).
- Neal, C. R., Crook, H., Bell, E., Harper, S. J. & Bates, D. O. Three-dimensional reconstruction of glomeruli by electron microscopy reveals a distinct restrictive urinary subpodocyte space. *J Am Soc Nephrol* **16**, 1223–1235, doi:10.1681/asn.2004100822 (2005).
- Nijenhuis, T. *et al.* Angiotensin II contributes to podocyte injury by increasing TRPC6 expression via an NFAT-mediated positive feedback signaling pathway. *Am J Pathol* **179**, 1719–1732, doi:10.1016/j.ajpath.2011.06.033 (2011).
- Peti-Peterdi, J., Burford, J. L. & Hackl, M. J. The first decade of using multiphoton microscopy for high-power kidney imaging. *Am J Physiol Renal Physiol* **302**, F227–233, doi:10.1152/ajprenal.00561.2011 (2012).
- Abdulreda, M. H. *et al.* High-resolution, noninvasive longitudinal live imaging of immune responses. *Proc Natl Acad Sci U S A* **108**, 12863–12868, doi:10.1073/pnas.1105002108 (2011).
- Appel, D. *et al.* Recruitment of podocytes from glomerular parietal epithelial cells. *J Am Soc Nephrol* **20**, 333–343 (2009).
- Smeets, B. *et al.* Tracing the origin of glomerular extracapillary lesions from parietal epithelial cells. *J Am Soc Nephrol* **20**, 2604–2615, doi:10.1681/asn.2009010122 (2009).
- Smeets, B. *et al.* Parietal epithelial cells participate in the formation of sclerotic lesions in focal segmental glomerulosclerosis. *J Am Soc Nephrol* **22**, 1262–1274, doi:10.1681/asn.2010090970 (2011).
- Kriz, W. Podocyte is the major culprit accounting for the progression of chronic renal disease. *Microsc Res Tech* **57**, 189–195 (2002).
- Salmon, A. H. *et al.* Evidence for restriction of fluid and solute movement across the glomerular capillary wall by the subpodocyte space. *Am J Physiol Renal Physiol* **293**, F1777–1786, doi:10.1152/ajprenal.00187.2007 (2007).
- Peti-Peterdi, J. Independent two-photon measurements of albumin GSC give low values. *Am J Physiol Renal Physiol* **296**, F1255–1257, doi:10.1152/ajprenal.00144.2009 (2009).
- Tojo, A. & Endou, H. Intrarenal handling of proteins in rats using fractional micropuncture technique. *Am J Physiol* **263**, F601–606 (1992).
- Tanner, G. A. Glomerular sieving coefficient of serum albumin in the rat: a two-photon microscopy study. *Am J Physiol Renal Physiol* **296**, F1258–1265, doi:10.1152/ajprenal.90638.2008 (2009).
- Hyink, D. P. *et al.* Endogenous origin of glomerular endothelial and mesangial cells in grafts of embryonic kidneys. *Am J Physiol* **270**, F886–899 (1996).
- Eremina, V. *et al.* Glomerular-specific alterations of VEGF-A expression lead to distinct congenital and acquired renal diseases. *J Clin Invest* **111**, 707–716 (2003).
- Kerjaschki, D. *et al.* Pathogenic antibodies inhibit the binding of apolipoproteins to megalin/gp330 in passive Heymann nephritis. *J Clin Invest* **100**, 2303–2309, doi:10.1172/jci119768 (1997).

Acknowledgments

We thank Dr. Susan E. Quaggin (Samuel Lunenfeld Research Institute, Toronto, Canada) for providing the NPHS1-CFP mice. A.D.K. was supported by a grant of the Swiss National



Science Foundation, a grant by the Swiss Society for Medical and Biological Scholarships and an Amgen-FROMO scholarship. A.F. is supported by the National Institute of Health (NIH) through the National Institute of Diabetes and Digestive and Kidney Diseases (NIDDK grant Number R01DK090316), by the Diabetes Research Institute Foundation (DRIF; diabetesresearch.org) and by the Peggy and Harold Katz Family Foundation. M.H.A. was supported by the NIH/NIDDK (grant number F32DK083226) and the DRIF.

Author contributions

A.D.K., A.C., A.F. and D.K. performed experiments. A.D.K., A.C., P.O.B., J.R. and A.F. designed the experiments. M.H.A. provided technical assistance during experiments and performed 3D reconstructions of images. C.F. provided transgenic animals. A.D.K. prepared all figures and wrote the main manuscript text. All authors reviewed the manuscript.

Additional information

Supplementary information accompanies this paper at <http://www.nature.com/scientificreports>

Competing financial interests: The authors declare no competing financial interests.

How to cite this article: Kistler, A.D. *et al.* In vivo imaging of kidney glomeruli transplanted into the anterior chamber of the mouse eye. *Sci. Rep.* **4**, 3872; DOI:10.1038/srep03872 (2014).



This work is licensed under a Creative Commons Attribution-NonCommercial-NoDerivs 3.0 Unported license. To view a copy of this license, visit <http://creativecommons.org/licenses/by-nc-nd/3.0>